CB1 and GLP-1 Receptors Cross Talk Provides New Therapies for Obesity

Philippe Zizzari,[1] Rongjun He,[2] Sarah Falk,[3] Luigi Bellocchio,[1] Camille Allard,[1] Samantha Clark,[1] Thierry Lesté-Lasserre,[1] Giovanni Marsicano,[1] Christoffer Clemmensen,[3] Diego Perez-Tilve,[4] Brian Finan,[2] Daniela Cota,[1] and Carmelo Quarta[1]

Diabetes 2021;70:415–422 | https://doi.org/10.2337/db20-0162

Glucagon-like peptide 1 receptor (GLP-1R) agonists effectively improve glycemia and body weight in patients with type 2 diabetes and obesity but have limited weight-lowering efficacy and minimal insulin sensitizing action. In preclinical models, peripherally restricted cannabinoid receptor type 1 (CB1R) inhibitors, which are devoid of the neuropsychiatric adverse effects observed with brain-penetrant CB1R blockers, ameliorate obesity and its multiple metabolic complications. Using mouse models with genetic loss of CB1R or GLP-1R, we demonstrate that these two metabolic receptors modulate food intake and body weight via reciprocal functional interactions. In diet-induced obese mice, the coadministration of a peripheral CB1R inhibitor with long-acting GLP-1R agonists achieves greater reduction in body weight and fat mass than monotherapies by promoting negative energy balance. This cotreatment also results in larger improvements in systemic and hepatic insulin action, systemic dyslipidemia, and reduction of hepatic steatosis. Thus, peripheral CB1R blockade may allow safely potentiating the antiobesity and antidiabetic effects of currently available GLP-1R agonists.

Few, and often subeffective, drugs are available to address the increasing prevalence of obesity and type 2 diabetes (1). Glucagon-like peptide 1 receptor (GLP-1R) agonists improve glycemic control (2) but show suboptimal efficacy against adiposity and insulin resistance (2–4). The first generation of brain-penetrant cannabinoid receptor type 1 (CB1R) antagonists displayed relevant body weight (BW)-lowering action but also caused neuropsychiatric adverse effects (5,6). Recently developed peripherally restricted CB1R inhibitors overcome these safety concerns, while potently lowering BW in animal models of obesity (7,8). These compounds also improve systemic and tissue-specific metabolic complications, including insulin and leptin resistance, dyslipidemia, nonalcoholic fatty liver disease, inflammation, β-cell loss, and diabetic nephropathy (6–10). Notably, GLP-1 secretion is modulated by changes in CB1R signaling (11), while the insulinotropic action of GLP-1R agonism is enhanced in mice lacking CB1R (12), suggesting the existence of reciprocal functional interactions between GLP-1R and CB1R.

Here we demonstrate that a cross talk between GLP-1R and peripheral CB1R signaling modulates food intake and BW. Coadministration of the peripheral CB1R blocker JD-5037 with GLP-1R agonists to diet-induced obese (DIO) mice has greater efficacy to lower BW than monotherapies, with superior and greater beneficial effects on insulin resistance, dyslipidemia, and hepatic steatosis. This combinatorial strategy may be used to correct obesity and its comorbidities and warrants further clinical investigation.

RESEARCH DESIGN AND METHODS

Animals and Treatments

The experiments were in compliance with European Union Directives (2010/63/EU), the University of Bordeaux Ethical Committee (DIR1354), and the University of Cincinnati

[1]University of Bordeaux, INSERM, Neurocentre Magendie, U1215, Bordeaux, France
[2]Novo Nordisk Research Center, Indianapolis, IN
[3]Novo Nordisk Foundation Center for Basic Metabolic Research, Faculty of Health and Medical Sciences, University of Copenhagen, Copenhagen, Denmark
[4]Department of Pharmacology and Systems Physiology, University of Cincinnati College of Medicine, Cincinnati, OH

Corresponding authors: Daniela Cota, daniela.cota@inserm.fr, and Carmelo Quarta, carmelo.quarta@inserm.fr

Received 16 February 2020 and accepted 27 October 2020

This article contains supplementary material online at https://doi.org/10.2337/figshare.13148288.

D.C. and C.Q. share last authorship.

Animal Care Committee. Male mice were housed at 22 ± 2°C (12 h dark/light cycle). CB1-knockout (*CB1*-KO) mice (13) were fed a regular chow diet (SAFE A03; SAFE diets). Eight-week-old male C57BL/6J mice (Janvier Laboratories, Le Genest-Saint-Isles, France) were fed a chow diet (SAFE A03) or a high-fat diet (HFD, D12492 or D12331; Research Diets) for 6 months before the study. GLP-1R-knockout (*GLP-1R*-KO) mice (14) were fed a HFD (D12331; Research Diets) for 16 weeks before the study. JD-5037 (#530481; MedKoo Biosciences) and rimonabant (9000484; Cayman Chemical) were given i.p., and IUB48 (14) or semaglutide (synthetized at Novo Nordisk Research Center of Indianapolis, IN) were given subcutaneously. JD-5037 was prepared in 0.9% NaCl with Tween 80 (1%) and DMSO (4%). Semaglutide was prepared in 50 mmol/L phosphate buffer (pH 7.4) with 0.05% Tween 80. Mice were randomly assigned to pharmacological treatment groups, and the experimenters were not blinded to the intervention groups. Animals were single housed or group housed, as specified in the figure legends.

Energy Expenditure

Energy expenditure was calculated using an energy balance technique (total energy expenditure balance [TEEbal]) (15).

Plasma and Tissues Analysis

Plasma insulin and leptin was determined by ELISA kit (Mercodia 10-1132-01 and 10-1113-01, and Millipore EZML-82K, respectively) and plasma and hepatic triglycerides by Thermo Scientific TR22421. For hepatic triglycerides extraction, livers (200 mg) were incubated overnight at 55°C in 30% ethanolic KOH. After 50% ethanol was added, they were centrifuged (13,000 rpm, 5 min), and 100 μL of $MgCl_2$ (1 mol/L) was added to 100 μL of supernatant. Samples were centrifuged again (13,000 rpm, 5 min) before quantification. Unknown triolein equivalents were interpolated using logistic regression. Triglycerides content was calculated in mg/g tissue by triolein equivalents * 2 * 0.012/(tissue weight in grams).

Body Composition Analysis

Body composition analysis was performed with an EchoMRI-900 (Echo Medical Systems).

Glucose Metabolism

Glucose tolerance, insulin tolerance, and glucose-induced insulin release were performed as previously described (14) using fasting durations and glucose/insulin concentrations detailed in the figure legends. The glucose disappearance rate (KITT) was calculated as the slope of the decreasing line of blood glucose levels over 30 min from insulin administration, as previously described (16).

Quantitative Real-time PCR

RNA tissue extraction and quantitative (q)PCR were performed as previously reported (17). Primers are provided in Supplementary Table 1.

Statistical Analyses

Data are mean ± SD and were analyzed using Prism 8 (GraphPad). ANOVA, followed by the appropriate post hoc test, was used as specified in the figure legends.

Data and Resource Availability Statement

All data and resources are available from the corresponding authors upon request.

RESULTS

CB1R and GLP-1R Interact to Control Food Intake but Not Glucose Tolerance

To explore possible functional interactions between CB1R and GLP-1R, we analyzed short-term changes in food intake and glycemic control in chow-fed *CB1*-KO or wild-type (WT) littermates acutely treated with multiple doses of a GLP-1R agonist (IUB48) (14) after 18 h of fasting, which activates the endocannabinoid system (18). At 10 nmol/kg, IUB48 suppressed food intake in both WT and *CB1*-KO mice, with a greater effect in the KO (Fig. 1*A*). A lower dose (0.5 nmol/kg) of IUB48 still reduced food intake in *CB1*-KO mice but not in WT controls (Fig. 1*B*). No genotype-dependent changes in systemic glucose tolerance were observed after testing several doses of IUB48 (Fig. 1*C* and Supplementary Fig. 1*A*). Accordingly, no changes in glucose-induced insulin release were observed after treatment with a low (0.1 nmol/kg) IUB48 dose (Supplementary Fig. 1*B*).

Next, we probed the effects of the coadministration of different doses of IUB48 and the CB1R antagonist rimonabant on fasting-induced food intake in chow-fed BL6 mice. Coadministration of appetite-suppressant doses of IUB48 and rimonabant reduced food intake to a greater extent relative to monotherapies (Fig. 1*D* and *E*). A greater hypophagic effect was also observed after cotreatment with an effective dose of IUB48 and a noneffective dose of rimonabant (Fig. 1*F*). Similarly, the combination of noneffective doses for both molecules reduced food intake in both refed (Fig. 1*G*) and free-fed (Supplementary Fig. 1*D*) animals. Thus, functional comodulation of CB1R and GLP-1R synergistically reduced food intake but did not impact acute changes in glycemic control.

Cotargeting of GLP-1R and CB1R Ameliorates DIO

Because peripheral CB1R antagonists have promising antiobesity and antidiabetes action (8), we tested the antiobesity effects of the combined chronic administration of IUB48 and the peripherally restricted CB1R inhibitor JD-5037 (7) in DIO mice. To uncover possible synergistic effects, we used a dose of JD-5037 (1 mg/kg) with subthreshold weight-lowering and hypophagic action (Supplementary Fig. 2*A*) and a dose of IUB48 (100 nmol/kg) with clear effects on insulin secretion but minimal efficacy against BW loss (14). As expected, 2 weeks of IUB48 monotherapy did not alter BW, food intake, or fat mass, whereas JD-5037 significantly reduced these parameters (7) (Fig. 2*A*–*C* and Supplementary Fig. 2*B*). The cotreatment

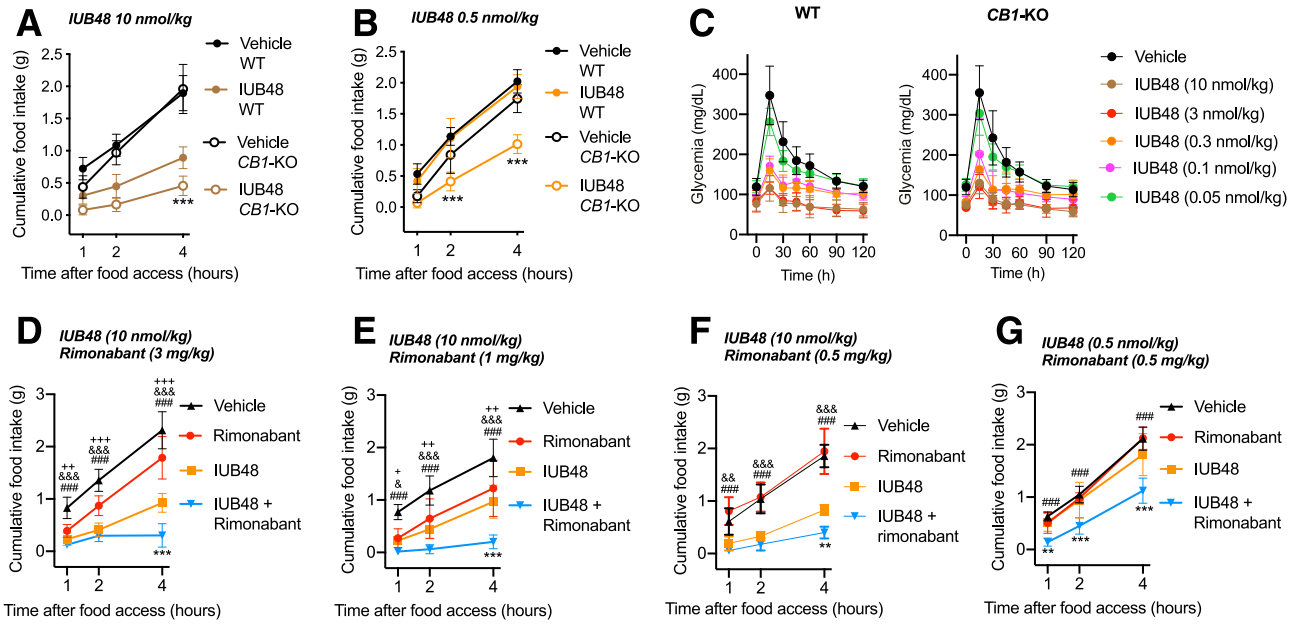

Figure 1—*A*: Fasting-induced cumulative food intake in WT and *CB1*-KO mice treated with vehicle or IUB48 (10 nmol/kg) 3 h before food access. The animals were fasted for 18 h before refeeding with regular chow diet. All mice were singly housed for at least 4 weeks before the start of the study and during the actual study ($n = 11$ per genotype or treatment, using a cross-over pharmacological design). Data were initially analyzed by three-way ANOVA. Genotype effect was $F(1, 60) = 34.31$, $P < 0.0001$; treatment × genotype effect was $F(1, 60) = 9.765$, $P = 0.0027$; and time × treatment × genotype effect was $F(2, 60) = 6.477$, $P = 0.0028$. Based on these results, we then performed two-way ANOVA analysis, followed by the Sidak multiple comparison test, at each individual time point. No genotype × treatment effect was observed at 1 h and 2 h of refeeding. However, a significant genotype × treatment effect was observed at 4 h ($F[1, 20] = 11.35$, $P = 0.0030$). Posttest: ***$P < 0.001$ comparing IUB48/WT vs. IUB48/*CB1*-KO. *B*: Fasting-induced cumulative food intake in WT and *CB1*-KO mice treated with vehicle or IUB48 (0.5 nmol/kg) 3 h before food access. The animals were fasted for 18 h before refeeding with regular chow diet. All mice were singly housed for at least 4 weeks before the start of the study and during the actual study ($n = 7$ per genotype or treatment, using a cross-over design). Data were initially analyzed by three-way ANOVA. Genotype effect was $F(1, 36) = 91.54$, $P < 0.0001$; treatment × genotype effect was $F(1, 36) = 27.11$, $P < 0.0001$; and time × treatment × genotype effect was $F(2, 36) = 8.279$; $P = 0.0011$. Based on these results, we then performed two-way ANOVA analysis, followed by the Sidak multiple comparison test, at each individual time point. No genotype × treatment effect was observed at 1 h. A significant genotype × treatment effect was observed at 2 h ($F[1, 12] = 9.210$; $P = 0.0104$) and 4 h of refeeding ($F[1, 12] = 31.55$; $P = 0.0001$). Posttest: ***$P < 0.001$ comparing IUB48/WT vs. IUB48/*CB1*-KO. *C*: Glucose tolerance test in 15 h-fasted WT or *CB1*-KO mice pretreated with vehicle or with different doses of IUB48, as indicated in the graph. All mice were singly housed for at least 4 weeks before the start of the study and during the actual study. Glucose (2 g/kg of lean mass) was injected i.p. The drug was administered 1 h before the glucose challenge. Data were obtained from three different cohorts of age-matched WT vs. *CB1*-KO littermates, and values relative to vehicle-treated mice were pooled to increase readability ($n = 7/12$ WT or *CB1*-KO mice were treated with the different doses of IUB48, $n = 30$ WT mice were treated with vehicle [pool of three cohorts], and $n = 27$ *CB1*-KO mice were treated with vehicle [pool of three cohorts]). *D*: Fasting-induced cumulative food intake in normal-weight C57BL/6J mice pretreated with vehicle, IUB48 (10 nmol/kg), rimonabant (3 mg/kg), or the combination of the two drugs 3 h before access to regular chow diet. Animals were fasted for 18 h before food access. All mice were singly housed for at least 4 weeks before the start of the study and during the actual study ($n = 6/9$ per group). Data were analyzed by two-way ANOVA repeated measurements with the Tukey multiple comparison test for individual time points. Treatment effect was $F(3, 27) = 93.31$, $P < 0.0001$, and time × treatment effect was $F(6, 54) = 23.68$, $P < 0.0001$. Posttest: ++$P < 0.01$ and +++$P <$ 0.001 comparing vehicle vs. rimonabant; &&&$P < 0.001$ comparing vehicle vs. IUB48; ###$P < 0.001$ comparing vehicle vs. IUB48 + rimonabant; ***$P < 0.001$ comparing IUB48 + rimonabant vs. monotherapies. *E*: Fasting-induced cumulative food intake in normal-weight C57BL/6J mice pretreated with vehicle, IUB48 (10 nmol/kg), rimonabant (1 mg/kg), or the combination of the two drugs 3 h before access to regular chow diet. Animals were fasted for 18 h before food access. All mice were singly housed for at least 4 weeks before the start of the study and during the actual study ($n = 5/6$ per group). Data were analyzed by two-way ANOVA repeated measurements with the Tukey multiple comparison test for individual time points. Treatment effect was $F(3, 18) = 23.40$, $P < 0.0001$, and time × treatment effect was $F(6, 36) = 7.512$, $P < 0.0001$. Posttest: +$P < 0.05$ and ++$P < 0.01$ comparing vehicle vs. rimonabant; &$P < 0.05$, &&&$P < 0.001$ comparing vehicle vs. IUB48; ###$P < 0.001$ comparing vehicle vs. IUB48 + rimonabant; ***$P < 0.001$ comparing IUB48 + rimonabant vs. monotherapies. *F*: Fasting-induced cumulative food intake in normal-weight C57BL/6J mice pretreated with vehicle, IUB48 (10 nmol/kg), rimonabant (0.5 mg/kg), or the combination of the two drugs 3 h before access to regular chow diet. Animals were fasted for 18 h before food access. All mice were singly housed for at least 4 weeks before the start of the study and during the actual study (n = 6 per group). Data were analyzed by two-way ANOVA repeated measurements with the Tukey multiple comparison test for individual time points. Treatment effect was $F(3, 20) = 45.02$, $P < 0.0001$, and time × treatment effect was $F(6, 40) = 16.49$, $P < 0.0001$. Posttest: &&$P < 0.01$ and &&&$P <$ 0.001 comparing vehicle vs. IUB48; ###$P < 0.001$ comparing vehicle vs. IUB48 + rimonabant; **$P < 0.01$ comparing IUB48 + rimonabant vs. monotherapies. *G*: Fasting-induced cumulative food intake in normal-weight C57BL/6J mice pretreated with vehicle, IUB48 (0.5 nmol/kg), rimonabant (0.5 mg/kg), or the combination of the two drugs 3 h before access to regular chow diet. Animals were fasted for 18 h before food access. All mice were singly housed for at least 4 weeks before the start of the study and during the actual study ($n = 8/9$ per group). Data were analyzed by two-way ANOVA repeated measurements with the Tukey multiple comparison test for individual time points. Treatment effect was $F(3, 31) = 27.26$, $P < 0.0001$, and time × treatment effect was $F(6, 62) = 6.543$, $P < 0.0001$. Posttest: ###$P < 0.001$ comparing vehicle vs. IUB48 + rimonabant, **$P < 0.01$ and ***$P < 0.001$ comparing IUB48 + rimonabant vs. monotherapies. All data are mean ± SD.

caused even greater reductions than monotherapies (Fig. 2*A–C*), without affecting lean mass (Fig. 2*C*), and also had greater hypophagic action than the monotherapies at day 1 and during week 2 (Fig. 2*B*), in agreement with our previous findings (Fig. 1).

JD-5037 reduced plasma leptin levels (Fig. 2*D*) and leptin mRNA expression in brown and white adipose tissues (Fig. 2*E*). The cotreatment caused similar or even greater reduction in these markers (Fig. 2*D* and *E*). No changes in systemic insulin action were found among treatments at day

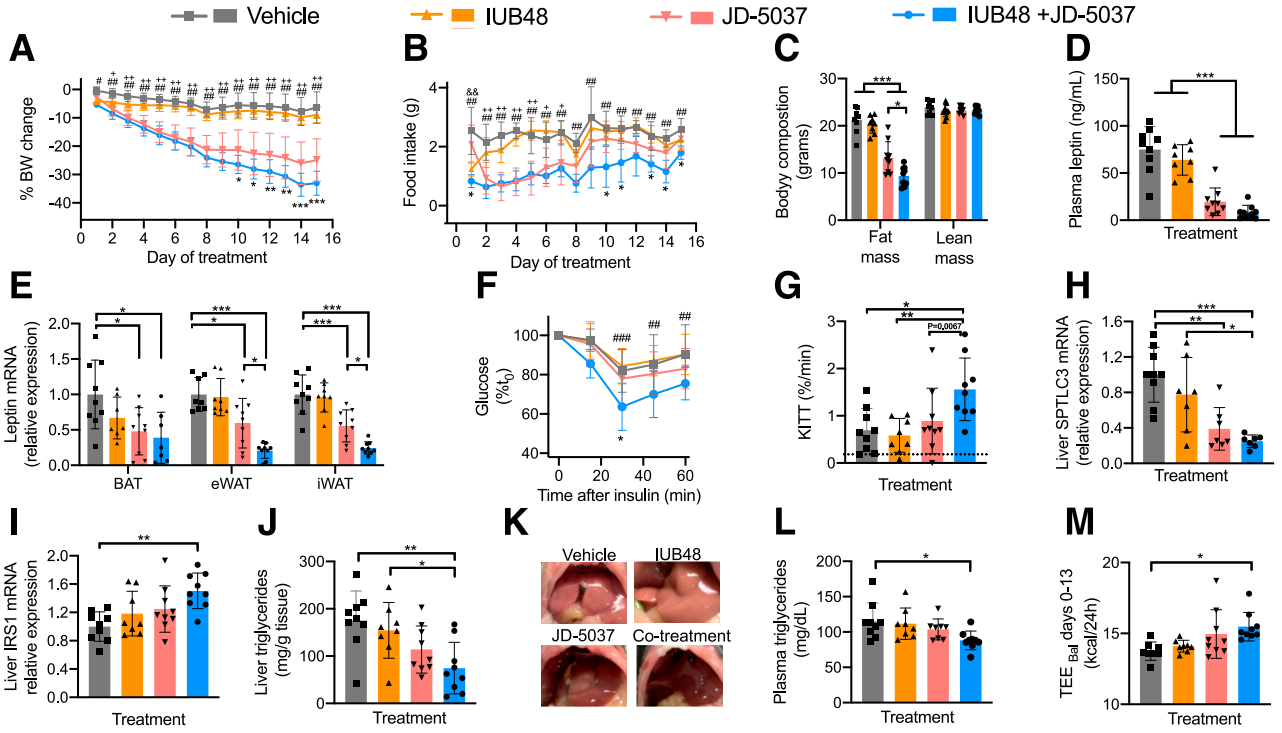

Figure 2—One cohort of C57BL6/J DIO mice treated with daily injections of vehicle (saline with 1% Tween and 4% DMSO i.p. + saline s.c.), JD-5037 (1 mg/kg of JD-5027 i.p. + saline s.c.), IUB48 (saline with 1% Tween and 4% DMSO i.p. + 100 nmol/kg of IUB48 s.c.), or the combination JD-5037 + IUB48 (1 mg/kg of JD-5037 i.p. + 100 nmol/kg of IUB48 s.c.) for 15 days (n = 8/9 mice per group). All mice were singly housed for at least 4 weeks before the start of the study and during the actual study. Effects on BW change (% change from day 0) (*A*) and daily food intake (grams) (*B*). Data were analyzed by two-way ANOVA repeated measurements with the Tukey multiple comparison test for individual time points. In *A*, treatment effect was $F(3, 31) = 57.97$, $P < 0.0001$ and time × treatment effect was $F(42, 434) = 22.04$, $P < 0.0001$. In *B*, treatment effect was $F(3, 31) = 47.55$, $P < 0.0001$, and time × treatment effect was $F(42, 434) = 4.692$, $P < 0.0001$. Posttest: ##$P < 0.01$ when comparing vehicle vs. IUB48 + JD-5037; +$P < 0.05$ and ++$P < 0.01$ when comparing vehicle vs. JD-5037; &&$P < 0.01$ when comparing vehicle vs. IUB48; *$P < 0.05$, **$P < 0.01$, and ***$P < 0.001$ when comparing IUB48 + JD-5037 vs. monotherapies. *C*: Effects on body composition at day 13 of treatment. Data were analyzed by one-way ANOVA (fat mass: $F[3, 31] = 43.12$, $P < 0.0001$; lean mass $F[3, 31] = 0.7254$, $P = 0.5446$], followed by the Tukey posttest. Posttest: *$P < 0.05$ and ***$P < 0.001$ as indicated in the graphs. *D*: Effects on plasma leptin level at day 15 of treatment. Data were analyzed by one-way ANOVA ($F[3, 31] = 33.52$, $P < 0.0001$) with the Tukey multiple comparison test. Posttest: ***$P < 0.001$ as indicated in the graph. *E*: Effects on leptin mRNA expression in brown adipose tissue (BAT), epididymal white adipose tissue (eWAT), and inguinal adipose tissue (iWAT). Data were analyzed by one-way ANOVA (BAT: $F[3, 28] = 4.223$, $P = 0.0139$; eWAT: $F[3, 30] = 18.07$, $P < 0.0001$; iWAT: $F[3, 31] = 25.49$, $P < 0.0001$) with the Tukey multiple comparison test. Posttest: *$P <$ 0.05 and ***$P < 0.001$ as indicated in the graph. *F*: Effects on insulin sensitivity (% change from basal glucose levels) at day 14 of treatment. The test was performed using 0.75 units/kg lean mass of insulin (Humulin, Eli Lilly) after 5 h of fasting. Data were analyzed by two-way ANOVA repeated measurements with the Tukey multiple comparison test for individual time points. Treatment effects was $F(3, 31) = 5.560$, $P =$ 0.0036 and time × treatment effect was $F(12, 124) = 2.215$, $P = 0.0147$. Posttest: ###$P < 0.001$ and ##$P < 0.01$ comparing vehicle vs. IUB48 + JD-5037; *$P < 0.05$ comparing IUB48 + JD-5037 vs. monotherapies. *G*: Effects on KITT from the analysis of insulin tolerance described in *F*. Data were analyzed by one-way ANOVA ($F[3, 31] = 5.224$, $P = 0.0049$) with the Tukey multiple comparison test. Posttest: *$P <$ 0.05 and **$P < 0.01$ as indicated in the graph. *H*: Effects on SPTLC3 mRNA levels analyzed by qPCR in livers collected at the end of the treatment. Data were analyzed by one-way ANOVA ($F[3, 26] = 10.98$, $P < 0.0001$) with the Tukey multiple comparison test. Posttest: *$P <$ 0.05, **$P < 0.01$ and ***$P < 0.001$ as indicated in the graph. *I*: Effects on IRS-1 mRNA levels analyzed by qPCR in livers collected at the end of the treatment. Data were analyzed by one-way ANOVA ($F[3, 31] = 5.022$, $P = 0.0059$) with the Tukey multiple comparison test. Posttest: **$P <$ 0.01 as indicated in the graph. *J*: Effects on tissue triglycerides content (mg of triglycerides/g of tissue) quantified in liver samples collected at the end of the treatment. Data were analyzed by one-way ANOVA ($F[3, 31] = 5.522$, $P = 0.0037$) with the Tukey multiple comparison test. Posttest: *$P < 0.05$, **$P < 0.01$ as indicated in the graph. *K*: Representative image showing fat deposition in the liver during necropsy after 15 days of the different treatments. *L*: Effects on plasma triglycerides levels (mg/dL) at day 15 of treatment. Data were analyzed by one-way ANOVA ($F[3, 30] = 3.3014$, $P = 0.0332$) with the Tukey multiple comparison test. Posttest: *$P < 0.05$ as indicated in the graph. *M*: Effects on estimated total energy expenditure (TEE) from days 0 to 13 of treatment using TEEbal analysis. Data were analyzed by one-way ANOVA ($F[3, 30] = 4.419$, $P = 0.0109$) with the Tukey multiple comparison test. Posttest: *$P < 0.05$ as indicated in the graphs. All data are mean ± SD.

8, as assessed by the analysis of the percentage blood glucose changes (Supplementary Fig. 2*C*) and by the KITT (Supplementary Fig. 2*D*). However, after 14 days, the cotreatment, but not monotherapies, significantly improved systemic insulin sensitivity (Fig. 2*F* and *G*). JD-5037–mediated effects on hepatic insulin resistance involve reduced hepatic content of ceramide via the lowered expression of the ceramide-producing enzyme SPTLC3 (9). Likewise, JD-5037 and JD-5037 + IUB48, but not IUB48 alone, reduced hepatic SPTLC3 mRNA expression after 2 weeks (Fig. 2*H*). This was paralleled by the increased hepatic expression of the insulin sensitivity marker IRS1 (Fig. 2*I*) and by a marked reduction in hepatic and systemic triglyceride levels in mice receiving the cotreatment (Fig. 2*J–L*).

The antiobesity action of the cotreatment was due to both food intake-dependent and -independent effects, since mice treated with IUB48 + JD-5037 had higher estimated energy expenditure relative to the vehicle (Fig. 2*M*). Consequently, animals pair-fed to the intake of mice receiving IUB48 + JD-5037 (Supplementary Fig. 2*E*) had less pronounced reductions in BW and fat mass than the cotreatment group (Supplementary Fig. 2*F* and *G*).

However, pair-feeding and the cotreatment similarly improved systemic insulin tolerance (Supplementary Fig. 2*H* and *I*). Thus, in response to combination therapy, compound-induced hypophagia is implicated in the observed ameliorations in insulin sensitivity, while mechanisms independent from food intake contribute to weight loss.

GLP-1R Is Necessary for the Weight-Lowering Action of the Peripheral CB1R Blocker JD-5037

Our data suggest that loss of CB1R function potentiates the hypophagic effects of GLP-1R agonism. However, the opposite relationship (i.e., a GLP-1R–mediated influence on CB1R signaling) could also be true. To address this second possibility, we tested the pharmacological efficacy of JD-5037 in *GLP-1R*-KO or WT littermates fed a HFD. After acute administration, JD-5037 did not modify the glycemic response to intraperitoneal or oral glucose loading in either WT or *GLP-1R*-KO mice (Fig. 3*A–C*). This is in agreement with the lack of functional interaction observed on acute glucose responses (Fig. 1*C*). However, the BW-lowering effect of JD-5037 was blunted in *GLP-1R*-KO animals (Fig. 3*D*), and this was reflected in a decreased hypophagic action of this molecule in *GLP-1R*-KO mice relative to WT controls (Fig. 3*E*). These results were not influenced by the initial BW differences between *GLP-1R*-KO and WT mice at day 0 of the study, since no correlations were found between these initial BW values and the BW changes induced by the drug (Fig. 3*F*). Thus, GLP-1R partially mediates the weight-lowering and hypophagic effects of JD-5037, which highlights the existence of a bidirectional cross talk between GLP-1R and CB1R signaling.

Pharmacological Potentiation of Semaglutide Efficacy Using Peripheral CB1-R Blockade

The long-acting GLP-1R agonist semaglutide shows greater glycemic benefits and a superior weight-lowering action than cognate molecules (2). To further investigate the therapeutic potential of GLP-1R and CB1R cotargeting, we assessed the efficacy of different doses of JD-5037 combined with one dose of semaglutide having submaximal BW-lowering effects (data not shown) in DIO mice. Semaglutide lowered BW, but it did not improve systemic insulin sensitivity relative to the vehicle, albeit it significantly lowered fasting blood glucose levels (Fig. 4 and Supplementary Fig. 3). Accordingly, the glycemic effects of GLP-1R agonists are not due to direct effects on systemic insulin action and are mainly due to improved insulin secretion and inhibition of glucagon production (3,4). When semaglutide was coadministered with a subthreshold dose of JD-5037 (0.3 mg/kg), which does not affect insulin sensitivity, this led to BW loss and to a significant improvement in insulin sensitivity relative to vehicle treatment, as assessed by the analysis of percentage blood glucose changes (Fig. 4*A*). Cotreatment of semaglutide with higher doses of JD-5037 (1 mg/kg and 3 mg/kg) caused greater BW loss than monotherapies (Fig. 4*B* and *C*). At these higher doses, the cotreatment and JD-5037 monotherapy, but not semaglutide, improved insulin sensitivity, as assessed by both the analysis of percentage blood glucose changes and by KITT analysis (Fig. 4*B* and *C*). The cotreatment at the higher doses also lowered basal blood glucose levels relative to vehicle administration (Supplementary Fig. 3*B* and *C*). Thus, the combination of JD-5037 with semaglutide causes superior weight loss and greater insulin-sensitizing effects than semaglutide monotherapy.

DISCUSSION

We report that GLP-1R and peripheral CB1R signaling interact in a bidirectional manner to control energy homeostasis. Blockade of CB1R potentiates GLP-1–mediated effects on food intake and fat mass, whereas GLP-1R signaling is partially required for endocannabinoid-mediated actions on energy balance, because the weight loss induced by peripheral CB1 blockade is blunted in *GLP-1R*-KO mice. Such a cross talk can be pharmacologically manipulated to achieve potent antiobesity and antidiabetic solutions, and this may have clinical implications. Based on our data, the addition of peripheral CB1R inhibitors to currently available GLP-1R mimetics may allow potent weight loss and larger improvements in insulin resistance, systemic dyslipidemia, and nonalcoholic fatty liver disease, relative to monotherapies, without inducing the neuropsychiatric alterations observed with brain-penetrant CB1R antagonists (6,7). This approach could be also effective against nonalcoholic steatohepatitis, which still lacks adequate medical treatments, a possibility supported by the potent reduction in hepatic lipid accumulation observed herein, by the known ability of JD-5037 to attenuate liver fibrosis in preclinical models (19) and by on-going or recently terminated clinical trials investigating the use of both CB1R inhibitors and semaglutide on this liver dysfunction.

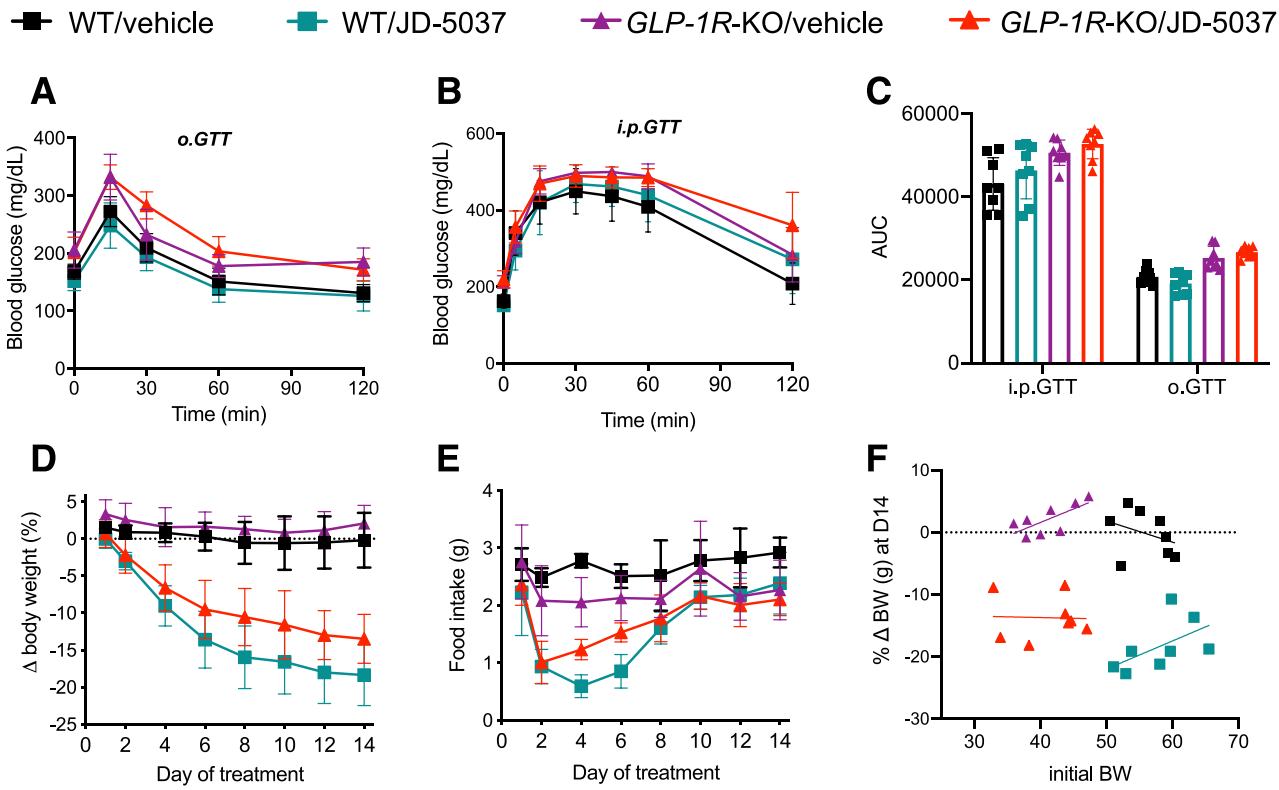

Figure 3—*A*: Effects on glucose tolerance (oral glucose tolerance test [o.GTT]) in one cohort of DIO-WT or DIO-*GLP-1R*-KO mice acutely treated with JD-5037 (3 mg/kg) 30 min before glucose administration. The dose of glucose injected during the test was 1.5 g/kg BW for *GLP-1R*-KO mice and 2.5 g/kg BW for WT mice. The animals were housed as $n = 2$ per cage during the test. Such a housing paradigm was setup at least 4 weeks before the start of the study ($n = 8$ per treatment or genotype). *B*: Effects on glucose tolerance (i.p. glucose tolerance test [i.p.GTT]) in one cohort of DIO-WT or DIO-*GLP-1R*-KO mice acutely treated with JD-5037 (3 mg/kg) 30 min before glucose administration. The dose of glucose injected during the test was 1.5 g/kg BW for *GLP-1R*-KO mice and 2.5 g/kg BW for WT mice. The animals were housed as $n = 2$ per cage during the study, using an equal number of cages ($n = 4$) per genotype or treatment group. Such a housing paradigm was setup at least 4 weeks before the start of the study and was maintained throughout the entire duration of the study ($n = 8$ per treatment or genotype). *C*: Glucose area under the curve (AUC) relative to the experiments described in *A* and *B*. Data were analyzed by two-way ANOVA. For i.p.GTT, genotype effect was $F(1, 28) = 14.05$, $P = 0.0008$, but no significant changes were detected in treatment effect ($F[1, 28] = 2.114$, $P = 0.1570$) or genotype × treatment effect ($F[1, 28] = 0.1107$, $P = 0.7418$). For o.GTT, genotype effect was $F(1, 28) = 61.01$, $P < 0.0001$, but no significant changes were detected in treatment effect ($F[1, 28] = 0.01105$, $P = 0.9170$) or genotype × treatment effect ($F[1, 28] = 3.861$, $P = 0.0594$). *D*: Effects on BW (% of change) in the DIO WT or DIO *GLP-1R*-KO mice described in *B*. *B*: After the GTT (day 0), the animals were chronically treated for the subsequent 14 days with vehicle or JD-5037 (3 mg/kg) once daily. Data were analyzed by three-way ANOVA. Treatment × genotype effect was significant: $F(1, 224) = 6.961$, $P = 0.0089$; genotype effect was significant: $F(1, 224) = 47.98$, $P < 0.0001$; and treatment effect was significant: $F(1, 224) = 891.3$, $P < 0.0001$. Time × treatment × genotype effect was not significant: $F(7, 224) = 0.8274$, $P = 0.5655$, preventing further post hoc analysis. *E*: Effects on daily food intake in the same cohort of DIO WT or DIO *GLP-1R*-KO mice in *B*. Data were analyzed by three-way ANOVA ($n = 4$ independent food intake measures per group were obtained by the average amount of food daily consumed in each cage divided by the number of animals per cage [$n = 2$]). Treatment × genotype effect was significant: $F(1, 96) = 15.47$, $P = 0.0002$. Genotype effect was not significant: $F(1, 96) = 3.203$, $P = 0.0767$; treatment effects was significant: $F(1, 96) = 118.0$, $P < 0.0001$; and time × genotype × treatment effect was not significant: $F(7, 96) = 1.118$, $P = 0.3583$, preventing further post hoc analysis. *F*: Correlation analysis between the initial BW values (day 0 of treatment) of the animals indicated in *D* and *E* and the percentage of BW change at day 14 (D14) of treatment. No significant correlations were found in any of the groups analyzed, as assessed by the Pearson correlation. All data (except *F*) are mean ± SD.

The greater efficacy observed with GLP-1R and CB1R comodulation likely results from multiple mechanisms that involve both food intake reduction and increased energy dissipation. JD-5037 may amplify the anorectic activity of GLP-1 (or vice versa) via periphery-to-brain signals involving the vagus nerve, which coexpress CB1R and GLP-1R (20) thus contributing to the hypophagic effects of CB1R inhibitors (18). The antiobesity effects of JD-5037 derive from changes in both food intake and energy expenditure (6,7), and these changes are due to restoration of endogenous leptin sensitivity (7,21,22) and lowered leptin production from adipocytes (7,22) via blockade of adipocytes CB1R (6,23). These same processes may be implicated in the antiobesity effects observed herein, since our cotreatment led to profound reductions in both circulating leptin levels and production. JD-5037 ameliorates insulin resistance via inhibition of hepatic CB1R (9) and via reduced accumulation of hepatic

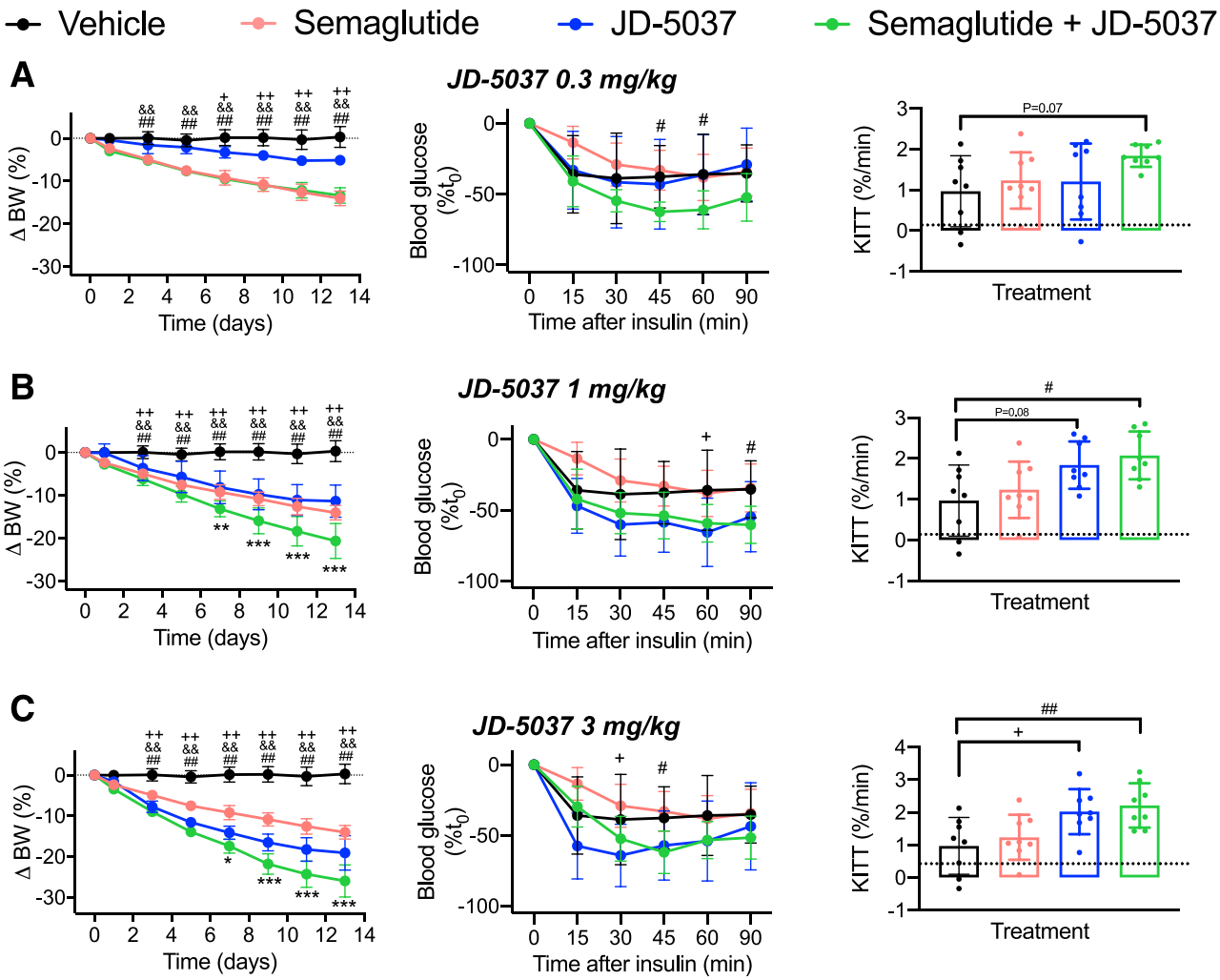

Figure 4—One cohort of DIO mice was treated daily with vehicle, semaglutide (1 nmol/kg), different does of JD-5037 (as indicated in the panels), or with the combination of the two drugs for 14 days. We analyzed the effect of these treatments on BW change (%) over time and insulin tolerance at day 14 of the study. Insulin tolerance was expressed as blood glucose change (% of t_0) or as KITT. During the insulin tolerance test, we injected 0.75 units/kg BW of insulin (Humulin, Eli Lilly) in animals fasted for 5 h (n = 8 mice per group). The visual and statistical representation of the different groups have been separated in different panels (*A–C*) corresponding to different doses of JD-5037 (0.3 mg/kg, 1 mg/kg, 3 mg/kg) to increase the readability of the results. BW changes were analyzed by two-way ANOVA repeated measurements with the Tukey multiple comparison test for individual time points (treatment effect: $F[7, 56] = 74.60$, $P < 0.0001$; time × treatment effect: $F[49, 392] = 38.39$, $P < 0.0001$). Blood glucose (% of t_0) values were analyzed by two-way ANOVA repeated measurements with the Dunnett test for the comparisons between treatments vs. vehicle at individual time points (treatment effect: $F[7, 58] = 2.560$, $P = 0.0228$; time × treatment effect: $F[35, 290] = 2.588$, $P < 0.0001$). KITT values were analyzed by one-way ANOVA ($F[7, 56] = 3.484$, $P = 0.0036$) with the Dunnett test for comparisons between treatments vs. vehicle. Posttest results were #$P < 0.05$ and ##$P < 0.01$ comparing vehicle vs. semaglutide + JD-5037; &&$P < 0.01$ comparing vehicle vs. semaglutide; +$P < 0.05$ and ++$P < 0.01$ comparing vehicle vs. JD-5037; *$P < 0.05$, **$P < 0.01$, and ***$P < 0.001$ comparing semaglutide + JD-5037 vs. monotherapies (n = 8 mice per group). All data are mean ± SD.

ceramide species interfering with insulin action (9,21). This mechanism, which involves an inhibitory effect on the ceramide-producing enzyme SPTLC3 (9), may be engaged by our cotreatment, which lowers hepatic SPTLC3 expression and improves markers of systemic and hepatic insulin action.

Thus, multiple neuronal and nonneuronal peripheral cell types expressing CB1R and GLP-1R may be involved in the antiobesity effects observed. A limitation of our work is that we do not dissect the exact identity of these peripheral sites of actions, which will require follow-up investigations.

Obesity is a heterogeneous disease requiring pharmacological approaches able to target multiple pathways. Unimolecular GLP-1R–based multiagonists affecting multiple metabolic targets have exceptional preclinical efficacy (4,14) and are being investigated in clinical studies. Chemical coupling of these newly developed molecules with a growing number of peripheral CB1R inhibitors (8) may have a transformative impact in obesity and diabetes pharmacotherapy, an exciting perspective given the structural and functional plasticity of CB1R (24) and the

emergence of novel generations of "fusion" peripheral CB1R inhibitors (8).

Acknowledgments. The authors thank the animal facility, genotyping, and transcriptome platforms of the INSERM U1215 NeuroCentre Magendie, funded by INSERM and LabEx Bordeaux Region Aquitaine Initiative for Neurosciences (BRAIN) (ANR-10-LABX-43), for animal care, mouse genotyping, and qPCR analyses. In particular, the help of Delphine Gonzales (Neurocentre Magendie, U1215, Bordeaux), Fiona Corailler (Neurocentre Magendie, U1215, Bordeaux), Helizabeth Huc (Neurocentre Magendie, U1215, Bordeaux), and Helene Doat (Neurocentre Magendie, U1215, Bordeaux) is acknowledged. The authors thank Charlotte Svendsen (Novo Nordisk Foundation Center for Basic Metabolic Research, Faculty of Health and Medical Sciences, University of Copenhagen, Denmark) for excellent laboratory support.

Funding. C.C. is supported by research grants from the Lundbeck Foundation (Fellowship R238-2016-2859) and the Novo Nordisk Foundation (grant number NNF17OC0026114). D.C. and C.Q. are supported by INSERM. D.C. is also supported by Nouvelle Aquitaine Region, LabEx Bordeaux Region Aquitaine Initiative for Neurosciences (BRAIN) (ANR-10-LABX-43), and Agence Nationale de la Recherche (ANR-10-EQX-008-1 OPTOPATH, ANR-17-CE14-0007 BABrain, and ANR-18-CE14-0029 Mitobesity). C.Q. is also supported by the Francophone Society of Diabetes (SFD), the French Society of Endocrinology (SFE), and the French Society of Nutrition (SFN). Novo Nordisk Foundation Center for Basic Metabolic Research is an independent Research Center, based at the University of Copenhagen, Denmark, and partially funded by an unconditional donation from the Novo Nordisk Foundation (www.cbmr.ku.dk) (grant number NNF18CC0034900).

Duality of Interest. B.F. and R.H. are current employees of Novo Nordisk. D.C. and G.M. are cofounder and stakeholders of the biotech Aelis Farma. D.P.-T. maintains research collaborations and receives funding from Novo Nordisk, Cohbar Inc., and MBX Biosciences Inc. No other potential conflicts of interest relevant to this article were reported.

Author Contributions. P.Z. performed most of the studies and analyzed data. R.H., S.F., L.B., C.A., S.C., T.L.-L., G.M., C.C., and D.P.-T. performed studies, analyzed data, and gave critical inputs. B.F., D.C., and C.Q. conceptualized and designed the experiments, analyzed data, and wrote the manuscript. C.Q. is the guarantor of this work and, as such, had full access to all the data in the study and takes responsibility for the integrity of the data and the accuracy of the data analysis.

References

1. Afshin A, Forouzanfar MH, Reitsma MB, et al.; GBD 2015 Obesity Collaborators. Health effects of overweight and obesity in 195 countries over 25 years. N Engl J Med 2017;377:13–27

2. Pratley RE, Aroda VR, Lingvay I, et al.; SUSTAIN 7 investigators. Semaglutide versus dulaglutide once weekly in patients with type 2 diabetes (SUSTAIN 7): a randomised, open-label, phase 3b trial. Lancet Diabetes Endocrinol 2018;6:275–286

3. Fonseca VA, Capehorn MS, Garg SK, et al. Reductions in insulin resistance are mediated primarily via weight loss in subjects with type 2 diabetes on semaglutide. J Clin Endocrinol Metab 2019;104:4078–4086

4. Müller TD, Clemmensen C, Finan B, DiMarchi RD, Tschöp MH. Anti-obesity therapy: from rainbow pills to polyagonists. Pharmacol Rev 2018;70:712–746

5. Christensen R, Kristensen PK, Bartels EM, Bliddal H, Astrup A. Efficacy and safety of the weight-loss drug rimonabant: a meta-analysis of randomised trials. Lancet 2007;370:1706–1713

6. Quarta C, Cota D. Anti-obesity therapy with peripheral CB1 blockers: from promise to safe(?) practice. Int J Obes 2020;44:2179–2193

7. Tam J, Cinar R, Liu J, et al. Peripheral cannabinoid-1 receptor inverse agonism reduces obesity by reversing leptin resistance. Cell Metab 2012;16:167–179

8. Cinar R, Iyer MR, Kunos G. The therapeutic potential of second and third generation CB_1R antagonists. Pharmacol Ther 2020;208:107477

9. Cinar R, Godlewski G, Liu J, et al. Hepatic cannabinoid-1 receptors mediate diet-induced insulin resistance by increasing de novo synthesis of long-chain ceramides. Hepatology 2014;59:143–153

10. Jourdan T, Godlewski G, Cinar R, et al. Activation of the Nlrp3 inflammasome in infiltrating macrophages by endocannabinoids mediates beta cell loss in type 2 diabetes. Nat Med 2013;19:1132–1140

11. Chia CW, Carlson OD, Liu DD, González-Mariscal I, Santa-Cruz Calvo S, Egan JM. Incretin secretion in humans is under the influence of cannabinoid receptors. Am J Physiol Endocrinol Metab 2017;313:E359–E366

12. González-Mariscal I, Krzysik-Walker SM, Kim W, Rouse M, Egan JM. Blockade of cannabinoid 1 receptor improves GLP-1R mediated insulin secretion in mice. Mol Cell Endocrinol 2016;423:1–10

13. Marsicano G, Goodenough S, Monory K, et al. CB1 cannabinoid receptors and on-demand defense against excitotoxicity. Science 2003;302:84–88

14. Quarta C, Clemmensen C, Zhu Z, et al. Molecular integration of incretin and glucocorticoid action reverses immunometabolic dysfunction and obesity. Cell Metab 2017;26:620–632.e6

15. Ravussin Y, Gutman R, LeDuc CA, Leibel RL. Estimating energy expenditure in mice using an energy balance technique. Int J Obes 2013;37:399–403

16. Alquier T, Poitout V. Considerations and guidelines for mouse metabolic phenotyping in diabetes research. Diabetologia 2018;61:526–538

17. Cardinal P, Bellocchio L, Clark S, et al. Hypothalamic CB1 cannabinoid receptors regulate energy balance in mice. Endocrinology 2012;153:4136–4143

18. Mazier W, Saucisse N, Gatta-Cherifi B, Cota D. The endocannabinoid system: pivotal orchestrator of obesity and metabolic disease. Trends Endocrinol Metab 2015;26:524–537

19. Tan S, Liu H, Ke B, Jiang J, Wu B. The peripheral CB 1 receptor antagonist JD5037 attenuates liver fibrosis via a CB 1 receptor/β-arrestin1/Akt pathway. Br J Pharmacol 2020;177:2830–2847

20. Egerod KL, Petersen N, Timshel PN, et al. Profiling of G protein-coupled receptors in vagal afferents reveals novel gut-to-brain sensing mechanisms. Mol Metab 2018;12:62–75

21. Liu J, Godlewski G, Jourdan T, et al. Cannabinoid-1 receptor antagonism improves glycemic control and increases energy expenditure through sirtuin-1/mechanistic target of rapamycin complex 2 and 5'adenosine monophosphate-activated protein kinase signaling. Hepatology 2019;69:1535–1548

22. Tam J, Szanda G, Drori A, et al. Peripheral cannabinoid-1 receptor blockade restores hypothalamic leptin signaling. Mol Metab 2017;6:1113–1125

23. Ruiz de Azua I, Mancini G, Srivastava RK, et al. Adipocyte cannabinoid receptor CB1 regulates energy homeostasis and alternatively activated macrophages. J Clin Invest 2017;127:4148–4162

24. Hua T, Vemuri K, Nikas SP, Laprairie RB, Wu Y, Qu L, et al. Crystal structures of agonist-bound human cannabinoid receptor CB1. Nature 2017;547:468–471